

# Accurate Prediction of Core Level Binding Energies from Ground-State Density Functional Calculations: The Importance of Localization and Screening

Jincheng Yu,<sup>†</sup> Yuncai Mei,<sup>†</sup> Zehua Chen,<sup>†,‡</sup> and Weitao Yang<sup>\*,†,¶</sup>

<sup>†</sup>*Department of Chemistry, Duke University, Durham, NC 27708, USA*

<sup>‡</sup>*Theoretical Chemistry Institute and Department of Chemistry, University of  
Wisconsin-Madison, Madison, WI 53706, USA*

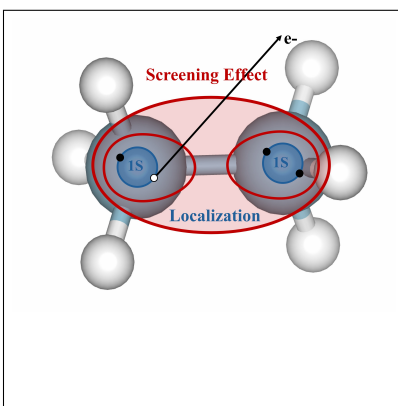
<sup>¶</sup>*Department of Physics, Duke University, Durham, NC 27708, USA*

E-mail: weitao.yang@duke.edu

## Abstract

A new method for predicting core level binding energies (CLBEs) is developed by both localizing the core-level states and describing the screening effect. CLBEs contain important information about the electronic structure, elemental chemistry, and chemical environment of molecules and materials. Theoretical study of CLBEs can provide insights for analyzing and interpreting the experimental results obtained from the X-ray photoelectron spectroscopy, in which the overlapping of signals is very common. The localization of core-level holes is important for the theoretical calculation of CLBEs. Predicting CLBEs from commonly used density functional approximations (DFAs) is challenging, because conventional DFAs often produce delocalized core-level states, especially when degenerate core-level states exist. In this work, we combine the localization procedure from the localized orbital scaling correction method and the curvature matrix generalized from the exact second-order correction method that contains the screening effect, and the resulting approach can accurately predict CLBEs from ground-state density functional calculations.

## TOC Graphic



Core-level binding energies (CLBEs), which are element-specific and sensitive to the chemical environment, are crucial for understanding the electronic properties, elemental chemistry, and oxidation state of molecules and materials.<sup>1,2</sup> Experimentally, CLBEs can be obtained from X-ray photoelectron spectroscopy (XPS).<sup>3-5</sup> However, due to the overlap between peaks on the spectrum, assigning XPS signals precisely to the atomic sites can be challenging, especially for complex materials.<sup>6</sup> Therefore, guidance from accurate theoretical analysis is often necessary for the interpretation of experimental results.<sup>2,7</sup>

Delta self-consistent field ( $\Delta$ SCF) method<sup>8</sup> is one of the earliest developed approaches to compute CLBEs with high accuracy. In  $\Delta$ SCF, CLBEs are calculated as the differences between the  $N$ -electron systems and the corresponding  $(N - 1)$ -electron systems with a core-level hole. In general, relative CLBEs from  $\Delta$ SCF are close to experimental results, with the deviations being around 0.2 eV for small systems.<sup>9</sup> While the deviation has a small dependence on the exchange-correlation (XC) functional, mean absolute errors (MAEs) from  $\Delta$ SCF are lower than 1 eV for most functionals.<sup>10-12</sup> Theoretically, calculating the binding energy by evaluating the total energies of the initial and final states remains challenging, particularly for bulk insulators.<sup>13</sup> After the emission of a photoelectron, the system becomes non-periodic due to the formation of a core-level hole. This disruption of periodicity complicates the use of conventional electronic structure methods that rely on periodic boundary conditions. Additionally, the Coulomb potential of the ionized bulk cannot be addressed under periodic assumptions due to Coulombic divergence. To address this issue, several methods have been developed, including neutralizing the final state by adding an electron into the conduction band,<sup>14-17</sup> approximating the bulk by a cluster model,<sup>18</sup> and using exact Coulomb cutoff method.<sup>13</sup> Numerical tests<sup>11,19-22</sup> indicate the high accuracy of  $\Delta$ SCF. Similar to  $\Delta$ SCF, other  $\Delta$  approaches<sup>23-32</sup> also require the explicit optimization of core-ionized or core-excited  $(N - 1)$ -electron systems.

In addition to traditional  $\Delta$  approaches, many methods based on response theories have also been developed to calculate CLBEs. These methods, including configuration interac-

tion methods,<sup>33–35</sup> equation-of-motion coupled-cluster methods,<sup>28,36</sup> and the Green’s function methods,<sup>37–45</sup> directly predict the charged excitation energies by calculating quasiparticle energies of the  $N$ -electron system. Thus, the numerically challenging optimization of the core-ionized state can be avoided. The  $GW$  method<sup>46</sup> is one of the most popular methods among these approaches. By replacing the bare Coulomb interaction to the dynamical screened interaction,  $GW$  has become a promising method to predict CLBEs for both solid-state and molecular systems.<sup>42,47–52</sup> Despite their great success, one-shot  $GW$  approaches have strong XC functional dependence,<sup>53</sup> making it difficult to find a XC functional that can provide accurate descriptions for both core-level and valence-level electronic structures.<sup>40,54</sup> Self-consistent approaches, such as  $evGW$  and  $scGW$ , can eliminate the XC functional dependence but significantly increase the computational cost.<sup>55–57</sup>

Approaches based on the density functional theory (DFT) have also been designed to predict CLBEs. Chong et al.<sup>58,59</sup> tested the performances of several generalized Slater’s transition-state (GSTS) models<sup>60,61</sup> using B88/P86 functional<sup>62,63</sup> and found that the unrestricted GSTS model provides the most accurate results. The statistical average of orbital potentials<sup>64–66</sup> was also applied to calculate CLBEs and achieved high accuracy. Crucially, the localization of core-level holes has been identified as a significant factor in calculating CLBEs.<sup>67</sup> More recently, a new method employing generalized Kohn-Sham (GKS) orbital energies derived from the random phase approximation energy functional with a semicanonical projection (d-GKS-spRPA) was developed.<sup>68</sup> This approach allows for the accurate determination of CLBEs from effective one-particle energies.

In this letter, we develop a new method for the accurate prediction of CLBEs from ground-state DFT calculations by considering both the localization of the core-level orbitals and the screening effect, within the framework of the localized orbital scaling correction (LOSC).<sup>69–71</sup>

The localization procedure and the curvature matrix capturing the screening interaction were both developed in the scaling correction (SC) methods<sup>69–71</sup> designed to eliminate

the delocalization error (DE)<sup>72–75</sup> in commonly used DFAs. For small or moderate systems with fractional charges, conventional DFAs violate the Perdew-Parr-Levy-Balduz (PPLB) linearity condition,<sup>76,77</sup> which states that the ground-state energy should be piecewise linear between integer points. Conventional DFAs typically produce convex curves, underestimating ground-state energies for fractional charge systems. For large systems, the convex deviation decreases, and the DE exists in another way, which results in too low relative ground-state energies for ionized systems. To systematically reduce the DE, researchers at the Yang laboratory developed various SC methods. The global scaling correction (GSC)<sup>78</sup> can restore the PPLB condition globally by correcting the convex curve for systems with fractional charges while preserving the ground-state energies for integer systems. However, GSC’s accuracy diminishes for larger systems where ground-state energies for integer systems are underestimated. To address this, the local scaling correction (LSC) method<sup>79</sup> was developed, applying the energy correction locally. The LOSC methods<sup>69,70,80–82</sup> combine GSC and LSC to achieve systematic improvement for descriptions of both small and large systems. More recently, the GSC2 method<sup>71</sup> was developed to capture exact second-order corrections to DFAs based on canonical molecular orbitals (CMOs), providing further improvement in descriptions of electronic structures of chemical systems. The GSC2 energy correction can be written as

$$\Delta_{\text{GSC2}}(\{n_{p\sigma}\}) = \frac{1}{2} \sum_{p\sigma} \frac{\partial^2 E(\{n_{m\tau}\})}{\partial n_{p\sigma}^2} (n_{p\sigma} - n_{p\sigma}^2), \quad (1)$$

where  $n_{p\sigma}$  is the occupation number for the  $p$ th orbital with spin  $\sigma$ , and  $E(\{n_{m\tau}\})$  is the energy of the system as a function of the set of occupation numbers  $\{n_{m\tau}\}$ . The second-order derivative can be evaluated using the Maxwell relationship and linear response theory<sup>71</sup>

$$\frac{\partial^2 E(\{n_{m\tau}\})}{\partial n_{p\sigma} \partial n_{q\sigma}} = \langle \psi_{p\sigma} \psi_{p\sigma}^* | K^{\sigma\sigma} + \sum_{\tau\nu} K^{\sigma\tau} \chi^{\tau\nu} K^{\nu\sigma} | \psi_{q\sigma} \psi_{q\sigma}^* \rangle, \quad (2)$$

where  $K^{\sigma\tau}$  represents Hartree-exchange-correlation kernels, and  $\chi^{\tau\mu}$  is the generalized linear response function.<sup>83,84</sup>

In connection to the chemical hardness,  $\frac{\partial^2 E(\{n_{m\tau}\})}{\partial n_{p\sigma}^2}$  is called the orbital hardness. To understand the physical meaning of the orbital hardness, we write the associated 4-point generalized dielectric function  $\varepsilon^{\sigma\tau}$  as  $(\varepsilon^{-1})^{\sigma\tau}(\mathbf{r}_1, \mathbf{r}_2, \mathbf{r}_3, \mathbf{r}_4) = \frac{\delta H_s^\sigma(\mathbf{r}_1, \mathbf{r}_2)}{\delta v^\tau(\mathbf{r}_3, \mathbf{r}_4)}$ . Now the expression in equation 2 leads to

$$W^{\sigma\zeta} = K^{\sigma\zeta} + \sum_{\tau\nu} K^{\sigma\tau} \chi^{\tau\nu} K^{\nu\zeta} = \sum_{\nu} (\varepsilon^{-1})^{\sigma\nu} K^{\nu\zeta} \quad (3)$$

equation 3 can be interpreted as the generalized screened interaction.<sup>71,85</sup>

In this letter, we combine the localization procedure from the LOSC and the screened interaction from the GSC2 to develop a new approach, linear-response LOSC (lrLOSC), for accurately predicting CLBES. The localization procedure is taken from the second version of LOSC (LOSC2),<sup>70</sup> which preserves the symmetry and the degeneracy of chemical systems. CMOs are linearly combined to minimize the cost function to ensure both physical and energy space localization:

$$F^\sigma = (1 - \gamma)F_r^\sigma + \gamma C F_e^\sigma, \quad (4)$$

where  $\gamma$  is set to be 0.707, and  $C$  is set to be 1000 (in atomic units).  $F_r^\sigma$  is the physical space cost function for spin  $\sigma$  taken from the Foster-Boys localization,<sup>86</sup>  $F_r^\sigma = \sum_{p\sigma} [\langle \phi_{p\sigma} | \mathbf{r}^2 | \phi_{p\sigma} \rangle - \langle \phi_{p\sigma} | \mathbf{r} | \phi_{p\sigma} \rangle^2]$ ,  $F_e^\sigma$  is the energy space cost function for spin  $\sigma$ ,  $F_e^\sigma = \sum_{p\sigma} [\langle \phi_{p\sigma} | \hat{h}^2 | \phi_{p\sigma} \rangle - \langle \phi_{p\sigma} | \hat{h} | \phi_{p\sigma} \rangle^2]$ , and  $\phi_{p\sigma}$  are orbitalets. Orbitalets are localized orbitals that are localized in multiple spaces obtained from linear combinations of both the occupied and the virtual CMOs,  $\phi_{p\sigma} = \sum_q U_{pq}^\sigma \psi_{q\sigma}$ . In practice, energy windows are often applied to select CMOs to reduce the computational cost.

The screening effect in lrLOSC is included by adopting the curvature matrix generalized from equation 2,

$$\kappa_{pq}^\sigma = \langle \phi_{p\sigma} \phi_{p\sigma}^* | K^{\sigma\sigma} + \sum_{\tau\nu} K^{\sigma\tau} \chi^{\tau\nu} K^{\nu\sigma} | \phi_{q\sigma} \phi_{q\sigma}^* \rangle. \quad (5)$$

Instead of CMOs, orbitalets are adopted in equation 5. equation 3 remains valid, ensuring

that the screening effect is accounted for in IrLOSC. Consequently, equation 4 and equation 5 lead to the following correction to the orbital energies:

$$\Delta\epsilon_{p\sigma} = \sum_i \kappa_{qq} \left( \frac{1}{2} - \lambda_{qq} \right) |U_{qp}^\sigma|^2 - \sum_{q \neq s} \kappa_{qs}^\sigma \lambda_{qs}^\sigma U_{qp}^\sigma U_{sp}^{\sigma*}, \quad (6)$$

where  $\lambda_{pq}^\sigma$  is the local occupation matrix. The correction to the total energy is

$$\Delta_{\text{IrLOSC}} = \frac{1}{2} \sum_{pq\sigma} \kappa_{pq}^\sigma \lambda_{pq}^\sigma (\delta_{pq} - \lambda_{pq}^\sigma) \quad (7)$$

CLBEs are approximated as effective one-particle energies following the methodology described in Refs. 68,87–89. Orbitals with energy differences of less than 0.05 eV are considered degenerate, and the quasihole energy  $\omega^-(N)$  describing the removal of one core-level electron from an  $N$ -electron system is approximated as the average of the degenerate orbital energies  $\{\epsilon_i(N)\}$ , i.e.

$$\omega^-(N) = E_0(N) - E(N-1) \approx \frac{1}{g} \sum_{i=1}^g \epsilon_i(N), \quad (8)$$

where  $g$  is the number of degenerate core-level orbitals,  $E_0(N)$  represents the ground-state energy of the  $N$ -electron system, and  $E(N-1)$  represents the energy of the  $(N-1)$ -electron system with a core-level hole.

The MAEs and the mean signed errors (MSEs) of absolute and relative CLBEs for different core species of systems from CORE65 test set<sup>90</sup> are shown in Table 1 and Table 2 respectively. The first thing we noticed is that MAEs from IrLOSC are the lowest in both the tables for all the functionals, indicating the ability of IrLOSC to improve the accuracy of CLBE calculations. The high accuracy of IrLOSC results is due to a) the proper localization of the core-level states and b) the well described screening effect.

We begin with the discussion of the influence of the localization procedure. As shown in Table 2, common DFAs can provide fairly accurate relative CLBEs. The MAEs from BLYP, B3LYP and PBE calculations are about 0.7 eV. However, common DFAs fail for absolute

CLBEs, as shown in Table 1, all studied DFAs underestimate the absolute CLBEs by over 15 eV. The fact that DFAs can provide much more accurate relative CLBEs than absolute CLBEs indicates that absolute CLBEs from DFA calculations need to be shifted. This shift can be achieved by correcting the DE. As shown by the MAEs and MSEs in Table 1, LOSC2<sup>70</sup> can shift the calculated CLBEs by around 30 eV. Overall, LOSC2 overestimate the absolute CLBEs by excessively shifting the energy levels. This is similar to the LOSC2 over correction for valence orbital energies for bulk systems.<sup>81</sup>

On the other hand, the localization procedure also plays an important role in the prediction of relative CLBEs. As tabulated in Table 2, the MAEs from LOSC2 calculations can be around 3 eV lower than those from GSC<sup>78</sup> calculations, and the MAEs from IrLOSC calculations are over 90% lower than those from GSC2<sup>71</sup> calculations. The localization is especially important for systems with degenerate core-level states. To further illustrate this, the errors of absolute and relative CLBEs from PBE calculations for 14 selected systems are plotted in Figure 1. Among these systems, C<sub>2</sub>H<sub>6</sub>, C<sub>6</sub>H<sub>6</sub>, (CH<sub>3</sub>)<sub>2</sub>CO, CF<sub>4</sub>, CHF<sub>3</sub>, CO<sub>2</sub> and O<sub>3</sub> have degenerate core-level states due to structural symmetry, while the degenerate core-level states of O<sub>2</sub> arises from the parent DFA calculation. For these systems, the localization of core-level holes is important for the calculation of CLBEs. However, the degenerate core-level orbitals from conventional DFT calculations can often be delocalized. Adding GSC or GSC2 corrections based on these delocalized orbitals leads to inaccurate results. We can take C<sub>2</sub>H<sub>6</sub> that has two degenerate core-level C1s states as an example. As shown in Figure 1 (b), the absolute errors from the GSC and the GSC2 calculations are significantly larger than those from the LOSC2 and the IrLOSC calculations. On the other hand, CH<sub>4</sub>, which shares similar size and chemical properties with C<sub>2</sub>H<sub>6</sub> but lacks degenerate core-level orbitals, has weaker dependency on the localization procedure. As shown in Figure 1 (a), for CH<sub>4</sub>, the errors from GSC and LOSC2 are similar, and the errors from GSC2 and IrLOSC are also very close. For C<sub>6</sub>H<sub>6</sub>, with an even greater number of degenerate states, the difference between GSC2 and IrLOSC results is more significant. For systems such as CO<sub>2</sub> and CHF<sub>3</sub>, although degenerate



core-level states exist, the corresponding atoms are not directly connected with a chemical bond. Therefore, the influence of the localization on these systems is less significant but still exists. Figure 1 (b) demonstrates that the delocalization nature of CMOs poses more significant issues in calculating relative CLBES. GSC and GSC2 results for systems with degenerate core-level states exhibit substantial deviations from the reference values.

Describing the screening effect is also very important for predicting CLBES. In GSC2 and IrLOSC, the screening effect is well captured by the curvature matrices as in equation 2 and equation 5 respectively. As shown in Table 1, both MAE and MSEs from GSC2 and IrLOSC are significantly lower than those from GSC and LOSC2. As a result, the overcorrection introduced by the localization procedure mentioned earlier can be significantly alleviated in IrLOSC. For each functional, the MAEs from IrLOSC are reduced to about one third of those from LOSC2. The importance of incorporating the screening effect is also shown by the plotted errors in Figure 1 (a), where the absolute heights of GSC2 and IrLOSC bars are much lower than those of GSC and LOSC2 bars. By effectively capturing the screening effect, IrLOSC also provides more accurate relative CLBES. For example, the MAE of B3LYP-IrLOSC is 0.14 eV, which is 0.46 eV lower than the MAE of B3LYP-LOSC2 results.

The screening effect is significantly more important for core-level orbitals compared to valence orbitals. This difference can be explained by considering the size and environment of the orbitals. Because the core-level orbitals are localized at the center of molecules and entirely surrounded by other orbitals, the removal of a core-level electron alters the environment for all other orbitals, which then relax or adjust to the formation of the core hole. This is the screening effect, which can be effectively captured with IrLOSC. In contrast, the effect is less pronounced for a valence hole, as valence shells are much larger and surrounded by only the vacuum outside molecules.

In summary, a new method, IrLOSC, has been developed for predicting CLBES based on ground-state DFT calculations. By incorporating both the localization of core-level holes and the screening effect, IrLOSC significantly improves the accuracy of CLBE predictions

compared to parent DFA calculations. The comparison of IrLOSC with LOSC2 and GSC2 results indicates that both the localization of core-level holes and the accurate description of screening effect are crucial for precise CLBE calculations. The localization procedure can introduce a positive energy shift on the basis of DFA calculations and is essential for predicting accurate relative CLBEs especially for systems with degenerate core-level states. Capturing the screening effect by incorporating the generalized GSC2 curvature matrix universally improves the prediction of both absolute and relative CLBEs. Building on the success of IrLOSC in calculating CLBEs, we plan to further investigate the effectiveness of IrLOSC in providing accurate valence and near-valence orbital energies, quasiparticle energies, and photoemission spectra in future studies.

**Table 1: MAEs of absolute CLBEs for different core atoms (in eV) of systems from CORE65 test set.<sup>90</sup> The calculations were performed using def2-TZVP basis set<sup>91</sup> with QM4D.<sup>92</sup>**

species	BLYP						B3LYP						PBE					
	A	B	C	D	E	F	A	B	C	D	E	F	A	B	C	D	E	F
C	21.86	8.88	8.74	3.74	2.87	2.98	14.48	8.87	10.02	3.26	2.86	2.98	22.56	8.30	8.04	3.34	2.34	2.46
F	32.27	14.60	14.62	3.46	3.47	4.18	21.32	9.14	16.20	4.86	2.78	3.49	33.00	13.94	13.89	6.15	2.76	3.47
N	24.50	11.59	11.54	3.65	3.15	3.39	15.95	11.34	12.89	3.20	2.84	3.07	25.07	11.13	10.97	3.30	2.69	2.93
O	27.83	13.99	14.65	5.42	3.42	3.84	18.03	13.75	16.12	4.33	2.92	3.35	28.45	13.80	13.95	4.85	2.86	3.29
MAE <sup>a</sup>	24.97	11.45	11.61	4.30	3.14	3.42	16.34	11.03	12.99	3.71	2.88	3.15	25.62	11.02	10.94	4.01	2.61	2.89
MSE <sup>a</sup>	-24.97	8.58	11.61	2.04	3.14	3.42	-16.34	8.96	12.99	1.60	2.88	3.15	-25.62	7.96	10.94	1.32	2.61	2.89

<sup>a</sup> The MAEs and the MSEs are calculated from CORE65 test set.<sup>90</sup> Nitrobenzene and phenylacetylene data are not calculated considering computational cost.

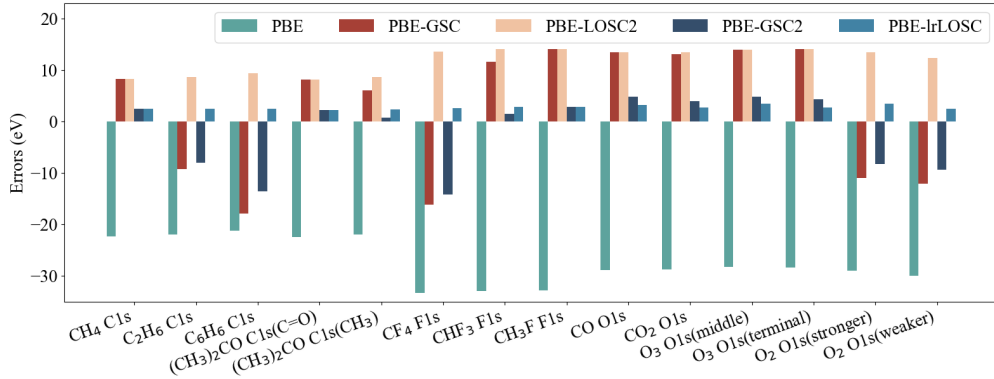
<sup>b</sup> A = KS-DFT, B = GSC, C = LOSC2, D = GSC2, E = lrLOSC, F = lrLOSC with relativistic correction.<sup>93</sup>

Table 2: MAEs of relative CLBEs for different core atoms (in eV) of systems from CORE65 test set.<sup>90</sup> The calculations were performed using def2-TZVP basis set<sup>91</sup> with QM4D.<sup>92</sup> The relative CLBE is defined as the energy difference relative to a reference molecule,  $\Delta E_{\text{relative}} = E_{\text{absolute}} - E_{\text{ref\_absolute}}$ .  $\text{CH}_4$ ,  $\text{NH}_3$ ,  $\text{H}_2\text{O}$  and  $\text{CH}_3\text{F}$  are the reference molecules for C1s, N1s, O1s and F1s respectively.

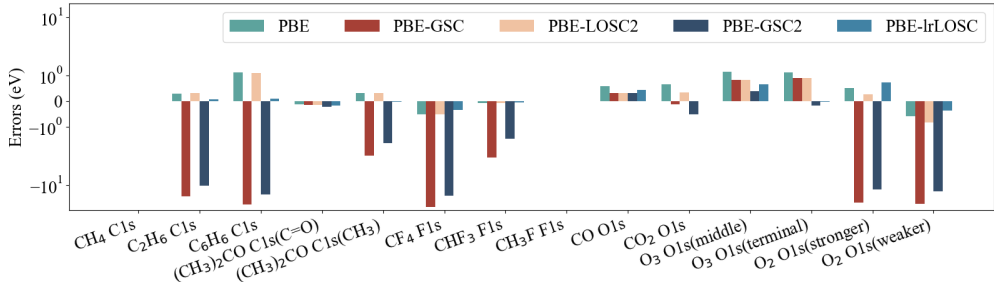
species	BLYP					B3LYP					PBE				
	A	B	C	D	E	A	B	C	D	E	A	B	C	D	E
C	0.52	3.68	0.52	2.06	0.14	0.41	3.49	0.41	1.67	0.11	0.55	3.78	0.56	2.13	0.16
F	0.17	0.19	0.17	0.11	0.10	0.12	12.78	0.12	5.78	0.07	0.19	10.94	0.19	6.16	0.13
N	0.62	2.68	0.62	1.22	0.10	0.64	3.88	0.64	1.56	0.05	0.69	2.73	0.69	1.21	0.06
O	0.99	4.24	0.80	2.06	0.20	1.03	4.58	0.86	1.79	0.22	1.04	3.27	0.86	1.51	0.22
MAE <sup>a</sup>	0.68	3.52	0.62	1.81	0.15	0.65	4.43	0.60	1.91	0.14	0.73	3.79	0.67	1.96	0.16
MAE <sup>a</sup>	0.28	-2.83	0.21	-1.78	-0.06	0.39	-3.71	0.32	-1.80	0.07	0.31	-3.01	0.23	-1.89	-0.01

<sup>a</sup> The MAEs and the MSEs are calculated from CORE65 test set.<sup>90</sup> Nitrobenzene and phenylacetylene data are not calculated considering computational cost.

<sup>b</sup> A = KS-DFT, B = GSC, C = LOSC2, D = GSC2, E = lrLOSC.



(a) errors of absolute CLBEs



(b) errors of relative CLBEs

Figure 1: Errors of (a) absolute and (b) relative CLBEs of systems from CORE65 test set. The calculations were done with PBE/def2-TZVP. The vertical axis of subfigure (b) uses symmetrical logarithmic scale.

## Acknowledgement

The authors acknowledge the support from the National Science Foundation (Grant No. CHE-2154831).

## Supporting Information Available

Detailed absolute and relative CLBEs from GSC, LOSEC2, GSC2, and IrLOSEC using different DFAs.

## References

- (1) Siegbahn, K. Electron Spectroscopy for Atoms, Molecules, and Condensed Matter. *Rev. Mod. Phys.* **1982**, *54*, 709–728.
- (2) Bagus, P. S.; Ilton, E. S.; Nelin, C. J. The Interpretation of XPS Spectra: Insights into Materials Properties. *Surf. Sci. Rep.* **2013**, *68*, 273–304.
- (3) Siegbahn, K.; Edvarson, K.  $\beta$ -Ray Spectroscopy in the Precision Range of 1 : 105. *Nucl. Phys.* **1956**, *1*, 137–159.
- (4) Siegbahn, K.; Nordling, C.; Fahlman, A.; Nordberg, R.; Hamrich, K.; Hednman, J.; Johansson, G.; Bergmark, J.; Karlsson, F.; Lindgren, I. et al. ESCA-Atomic, Molecular and Solid State Structure Studies by Means of Electron Spectroscopy, *Roy. Soc. Sci. Uppsala* **1967**, *20*.
- (5) Barr, T. L.; Modern, E. The principles and practice of X-ray photoelectron spectroscopy. *CRC, Boca Raton, FL* **1994**, 11.
- (6) Aarva, A.; Deringer, V. L.; Sainio, S.; Laurila, T.; Caro, M. A. Understanding X-ray Spectroscopy of Carbonaceous Materials by Combining Experiments, Density Func-

- tional Theory, and Machine Learning. Part I: Fingerprint Spectra. *Chem. Mater.* **2019**, *31*, 9243–9255.
- (7) Egelho, W. F. Core-Level Binding-Energy Shifts at Surfaces and in Solids. *Surf. Sci. Rep.* **1987**, *6*, 253–415.
- (8) Bagus, P. S. Self-Consistent-Field Wave Functions for Hole States of Some Ne-Like and Ar-Like Ions. *Phys. Rev.* **1965**, *139*, A619–A634.
- (9) Pueyo Bellafont, N.; Álvarez Saiz, G.; Viñes, F.; Illas, F. Performance of Minnesota Functionals on Predicting Core-Level Binding Energies of Molecules Containing Main-Group Elements. *Theor. Chem. Acc.* **2016**, *135*, 35.
- (10) Pueyo Bellafont, N.; Bagus, P. S.; Illas, F. Prediction of Core Level Binding Energies in Density Functional Theory: Rigorous Definition of Initial and Final State Contributions and Implications on the Physical Meaning of Kohn-Sham Energies. *J. Chem. Phys.* **2015**, *142*, 214102.
- (11) Kahk, J. M.; Lischner, J. Accurate Absolute Core-Electron Binding Energies of Molecules, Solids, and Surfaces from First-Principles Calculations. *Phys. Rev. Materials* **2019**, *3*, 100801.
- (12) Pueyo Bellafont, N.; Viñes, F.; Illas, F. Performance of the TPSS Functional on Predicting Core Level Binding Energies of Main Group Elements Containing Molecules: A Good Choice for Molecules Adsorbed on Metal Surfaces. *J. Chem. Theory Comput.* **2016**, *12*, 324–331.
- (13) Ozaki, T.; Lee, C.-C. Absolute Binding Energies of Core Levels in Solids from First Principles. *Phys. Rev. Lett.* **2017**, *118*, 026401.
- (14) Pehlke, E.; Scheer, M. Evidence for Site-Sensitive Screening of Core Holes at the Si and Ge (001) Surface. *Phys. Rev. Lett.* **1993**, *71*, 2338–2341.

- (15) Olovsson, W.; Marten, T.; Holmström, E.; Johansson, B.; Abrikosov, I. A. First principle calculations of core-level binding energy and Auger kinetic energy shifts in metallic solids. *J. Electron Spectrosc. and Relat. Phenom.* **2010**, *178*, 88–99.
- (16) Ljungberg, M.; Mortensen, J. J.; Pettersson, L. An implementation of core level spectroscopies in a real space projector augmented wave density functional theory code. *J. Electron Spectrosc. and Relat. Phenom.* **2011**, *184*, 427–439.
- (17) Susi, T.; Mowbray, D. J.; Ljungberg, M. P.; Ayala, P. Calculation of the graphene C 1s core level binding energy. *Phys. Rev. B* **2015**, *91*, 081401.
- (18) Bagus, P. S.; Ilton, E. S.; Nelin, C. J. The interpretation of XPS spectra: Insights into materials properties. *Surf. Sci. Rep.* **2013**, *68*, 273–304.
- (19) Kahk, J. M.; Lischner, J. Core Electron Binding Energies of Adsorbates on Cu(111) from First-Principles Calculations. *Phys. Chem. Chem. Phys.* **2018**, *20*, 30403–30411.
- (20) Pueyo Bellafont, N.; Viñes, F.; Hieringer, W.; Illas, F. Predicting Core Level Binding Energies Shifts: Suitability of the Projector Augmented Wave Approach as Implemented in VASP. *J. Chem. Phys.* **2017**, *38*, 518–522.
- (21) Olovsson, W.; Göransson, C.; Pourovskii, L. V.; Johansson, B.; Abrikosov, I. A. Core-Level Shifts in Fcc Random Alloys: A First-Principles Approach. *Phys. Rev. B* **2005**, *72*, 064203.
- (22) Köhler, L.; Kresse, G. Density Functional Study of CO on Rh(111). *Phys. Rev. B* **2004**, *70*, 165405.
- (23) Naves de Brito, A.; Correia, N.; Svensson, S.; Ågren, H. A Theoretical Study of X-ray Photoelectron Spectra of Model Molecules for Polymethylmethacrylate. *J. Chem. Phys.* **1991**, *95*, 2965–2974.

- (24) Ågren, H.; Jensen, H. J. A. Relaxation and Correlation Contributions to Molecular Double Core Ionization Energies. *Chem. Phys.* **1993**, *172*, 45–57.
- (25) Triguero, L.; Plashkevych, O.; Pettersson, L. G. M.; Ågren, H. Separate State vs. Transition State Kohn-Sham Calculations of X-ray Photoelectron Binding Energies and Chemical Shifts. *J. Electron Spectros. Relat. Phenomena* **1999**, *104*, 195–207.
- (26) Su, N. Q.; Xu, X. Second-Order Perturbation Theory for Fractional Occupation Systems: Applications to Ionization Potential and Electron Affinity Calculations. *J. Chem. Theory Comput.* **2016**, *12*, 2285–2297.
- (27) Miga, S.; Grabowski, I. Spin-Component-Scaled  $\Delta$ MP2 Parametrization: Toward a Simple and Reliable Method for Ionization Energies. *J. Chem. Theory Comput.* **2018**, *14*, 4780–4790.
- (28) Nooijen, M.; Bartlett, R. J. Description of Core-excitation Spectra by the Open-shell Electron-attachment Equation-of-motion Coupled Cluster Method. *J. Chem. Phys.* **1995**, *102*, 6735–6756.
- (29) Ohtsuka, Y.; Nakatsuji, H. Inner-Shell Ionizations and Satellites Studied by the Open-Shell Reference Symmetry-Adapted Cluster/Symmetry-Adapted Cluster Configuration-Interaction Method. *J. Chem. Phys.* **2006**, *124*, 054110.
- (30) Besley, N. A. Equation of Motion Coupled Cluster Theory Calculations of the X-ray Emission Spectroscopy of Water. *Chem. Phys. Lett.* **2012**, *542*, 42–46.
- (31) Sen, S.; Shee, A.; Mukherjee, D. Inclusion of Orbital Relaxation and Correlation through the Unitary Group Adapted Open Shell Coupled Cluster Theory Using Non-Relativistic and Scalar Relativistic Hamiltonians to Study the Core Ionization Potential of Molecules Containing Light to Medium-Heavy Elements. *J. Chem. Phys.* **2018**, *148*, 054107.

- (32) Zheng, X.; Cheng, L. Performance of Delta-Coupled-Cluster Methods for Calculations of Core-Ionization Energies of First-Row Elements. *J. Chem. Theory Comput.* **2019**, *15*, 4945–4955.
- (33) Asmuruf, F. A.; Besley, N. A. Calculation of Near-Edge X-ray Absorption Fine Structure with the CIS(D) Method. *Chem. Phys. Lett.* **2008**, *463*, 267–271.
- (34) Maganas, D.; DeBeer, S.; Neese, F. Restricted Open-Shell Configuration Interaction Cluster Calculations of the L-Edge X-ray Absorption Study of TiO<sub>2</sub> and CaF<sub>2</sub> Solids. *Inorg. Chem.* **2014**, *53*, 6374–6385.
- (35) Ehlert, C.; Klamroth, T. The Quest for Best Suited References for Configuration Interaction Singles Calculations of Core Excited States. *J. Comput. Chem.* **2017**, *38*, 116–126.
- (36) Liu, J.; Matthews, D.; Coriani, S.; Cheng, L. Benchmark Calculations of K-Edge Ionization Energies for First-Row Elements Using Scalar-Relativistic Core–Valence-Separated Equation-of-Motion Coupled-Cluster Methods. *J. Chem. Theory Comput.* **2019**, *15*, 1642–1651.
- (37) Barth, A.; Cederbaum, L. S. Many-Body Theory of Core-Valence Excitations. *Phys. Rev. A* **1981**, *23*, 1038–1061.
- (38) Barth, A.; Schirmer, J. Theoretical Core-Level Excitation Spectra of N<sub>2</sub> and CO by a New Polarisation Propagator Method. *J. Phys. B: At. Mol. Phys.* **1985**, *18*, 867–885.
- (39) Ekström, U.; Norman, P.; Carravetta, V.; Ågren, H. Polarization Propagator for X-Ray Spectra. *Phys. Rev. Lett.* **2006**, *97*, 143001.
- (40) Golze, D.; Keller, L.; Rinke, P. Accurate Absolute and Relative Core-Level Binding Energies from *GW*. *J. Phys. Chem. Lett.* **2020**, *11*, 1840–1847.



- (41) Zhu, T.; Chan, G. K.-L. All-electron Gaussian-based  $G_0W_0$  for valence and core excitation energies of periodic systems. *J. Chem. Theory Comput.* **2021**, *17*, 727–741.
- (42) Li, J.; Chen, Z.; Yang, W. Renormalized Singles Green's Function in the T-Matrix Approximation for Accurate Quasiparticle Energy Calculation. *J. Phys. Chem. Lett.* **2021**, *12*, 6203–6210.
- (43) Li, J.; Jin, Y.; Rinke, P.; Yang, W.; Golze, D. Benchmark of GW methods for core-level binding energies. *J. Chem. Theory Comput.* **2022**, *18*, 7570–7585.
- (44) Li, J.; Yang, W. Renormalized Singles with Correlation in GW Green's Function Theory for Accurate Quasiparticle Energies. *J. Phys. Chem. Lett.* **2022**, *13*, 9372–9380.
- (45) Li, J.; Yu, J.; Chen, Z.; Yang, W. Linear Scaling Calculations of Excitation Energies with Active-Space Particle–Particle Random-Phase Approximation. *J. Phys. Chem. A* **2023**, *127*, 7811–7822.
- (46) Hedin, L. New Method for Calculating the One-Particle Green's Function with Application to the Electron-Gas Problem. *Phys. Rev.* **1965**, *139*, A796–A823.
- (47) Ishii, S.; Ohno, K.; Kawazoe, Y.; Louie, S. G. *Ab Initio* GW Quasiparticle Energies of Small Sodium Clusters by an All-Electron Mixed-Basis Approach. *Phys. Rev. B* **2001**, *63*, 155104.
- (48) Rostgaard, C.; Jacobsen, K. W.; Thygesen, K. S. Fully Self-Consistent GW Calculations for Molecules. *Phys. Rev. B* **2010**, *81*, 085103.
- (49) Baumeier, B.; Andrienko, D.; Ma, Y.; Rohlfing, M. Excited States of Dicyanovinyl-Substituted Oligothiophenes from Many-Body Green's Functions Theory. *J. Chem. Theory Comput.* **2012**, *8*, 997–1002.
- (50) Caruso, F.; Rinke, P.; Ren, X.; Scheer, M.; Rubio, A. Unified Description of Ground

- and Excited States of Finite Systems: The Self-Consistent G W Approach. *Phys. Rev. B* **2012**, *86*, 081102.
- (51) Govoni, M.; Galli, G. Large Scale GW Calculations. *J. Chem. Theory Comput.* **2015**, *11*, 2680–2696.
- (52) Maggio, E.; Kresse, G. GW Vertex Corrected Calculations for Molecular Systems. *J. Chem. Theory Comput.* **2017**, *13*, 4765–4778.
- (53) Fuchs, F.; Furthmüller, J.; Bechstedt, F.; Shishkin, M.; Kresse, G. Quasiparticle Band Structure Based on a Generalized Kohn-Sham Scheme. *Phys. Rev. B* **2007**, *76*, 115109.
- (54) Dauth, M.; Caruso, F.; Kümmel, S.; Rinke, P. Piecewise Linearity in the G W Approximation for Accurate Quasiparticle Energy Predictions. *Phys. Rev. B* **2016**, *93*, 121115.
- (55) Caruso, F.; Rinke, P.; Ren, X.; Rubio, A.; Scheer, M. Self-Consistent G W : All-electron Implementation with Localized Basis Functions. *Phys. Rev. B* **2013**, *88*, 075105.
- (56) Caruso, F.; Dauth, M.; van Setten, M. J.; Rinke, P. Benchmark of GW Approaches for the GW 100 Test Set. *J. Chem. Theory Comput.* **2016**, *12*, 5076–5087.
- (57) Kaplan, F.; Harding, M. E.; Seiler, C.; Weigend, F.; Evers, F.; van Setten, M. J. Quasi-Particle Self-Consistent GW for Molecules. *J. Chem. Theory Comput.* **2016**, *12*, 2528–2541.
- (58) Chong, D. P. Accurate Calculation of Core-Electron Binding Energies by the Density-Functional Method. *Chem. Phys. Lett.* **1995**, *232*, 486–490.
- (59) Chong, D. P. Density-functional Calculation of Core-electron Binding Energies of C, N, O, and F. *J. Chem. Phys.* **1995**, *103*, 1842–1845.

- (60) Slater, J. *Advan. Quantum Chem.* **6** (1972) 1. DS. Choo, private communication. K. Schwa. *Phys. Rev. B* **1972**, *5*, 2466.
- (61) Williams, A. R.; deGroot, R. A.; Sommers, C. B. Generalization of Slater's Transition State Concept. *J. Chem. Phys.* **1975**, *63*, 628–631.
- (62) Becke, A. D. Density-Functional Exchange-Energy Approximation with Correct Asymptotic Behavior. *Phys. Rev. A* **1988**, *38*, 3098–3100.
- (63) Perdew, J. P. Density-Functional Approximation for the Correlation Energy of the Inhomogeneous Electron Gas. *Phys. Rev. B* **1986**, *33*, 8822–8824.
- (64) Chong, D. P.; Gritsenko, O. V.; Baerends, E. J. Interpretation of the Kohn–Sham Orbital Energies as Approximate Vertical Ionization Potentials. *J. Chem. Phys.* **2002**, *116*, 1760–1772.
- (65) Takahata, Y.; Chong, D. P. DFT Calculation of Core-Electron Binding Energies. *J. Electron Spectros. Relat. Phenomena* **2003**, *133*, 69–76.
- (66) Takahata, Y.; Wulfman, C. E.; Chong, D. P. Accurate Calculation of N1s and C1s Core Electron Binding Energies of Substituted Pyridines. Correlation with Basicity and with Hammett Substituent Constants. *J. Mol. Struct.* **2008**, *863*, 33–38.
- (67) Chong, D. P. Localized and Delocalized 1s Core-Holes in DFT Calculations. *J. Electron Spectros. Relat. Phenomena* **2007**, *159*, 94–96.
- (68) Voora, V. K.; Galhenage, R.; Hemminger, J. C.; Furche, F. Effective One-Particle Energies from Generalized Kohn–Sham Random Phase Approximation: A Direct Approach for Computing and Analyzing Core Ionization Energies. *J. Chem. Phys.* **2019**, *151*, 134106.

- (69) Li, C.; Zheng, X.; Su, N. Q.; Yang, W. Localized Orbital Scaling Correction for Systematic Elimination of Delocalization Error in Density Functional Approximations. *Natl. Sci. Rev.* **2018**, *5*, 203–215.
- (70) Su, N. Q.; Mahler, A.; Yang, W. Preserving Symmetry and Degeneracy in the Localized Orbital Scaling Correction Approach. *J. Phys. Chem. Lett.* **2020**, *11*, 1528–1535.
- (71) Mei, Y.; Chen, Z.; Yang, W. Exact Second-Order Corrections and Accurate Quasiparticle Energy Calculations in Density Functional Theory. *J. Phys. Chem. Lett.* **2021**, *12*, 7236–7244.
- (72) Cohen, A. J.; Mori-Sánchez, P.; Yang, W. Fractional Spins and Static Correlation Error in Density Functional Theory. *J. Chem. Phys.* **2008**, *129*, 121104.
- (73) Cohen, A. J.; Mori-Sánchez, P.; Yang, W. Insights into current limitations of density functional theory. *Science* **2008**, *321*, 792–794.
- (74) Mori-Sánchez, P.; Cohen, A. J.; Yang, W. Localization and Delocalization Errors in Density Functional Theory and Implications for Band-Gap Prediction. *Phys. Rev. Lett.* **2008**, *100*, 146401.
- (75) Cohen, A. J.; Mori-Sánchez, P.; Yang, W. Challenges for Density Functional Theory. *Chem. Rev.* **2012**, *112*, 289–320.
- (76) Perdew, J. P.; Parr, R. G.; Levy, M.; Balduz, J. L. Density-Functional Theory for Fractional Particle Number: Derivative Discontinuities of the Energy. *Phys. Rev. Lett.* **1982**, *49*, 1691–1694.
- (77) Yang, W.; Zhang, Y.; Ayers, P. W. Degenerate Ground States and a Fractional Number of Electrons in Density and Reduced Density Matrix Functional Theory. *Phys. Rev. Lett.* **2000**, *84*, 5172–5175.

- (78) Zheng, X.; Cohen, A. J.; Mori-Sánchez, P.; Hu, X.; Yang, W. Improving Band Gap Prediction in Density Functional Theory from Molecules to Solids. *Phys. Rev. Lett.* **2011**, *107*, 026403.
- (79) Li, C.; Zheng, X.; Cohen, A. J.; Mori-Sánchez, P.; Yang, W. Local Scaling Correction for Reducing Delocalization Error in Density Functional Approximations. *Phys. Rev. Lett.* **2015**, *114*, 053001.
- (80) Mei, Y.; Chen, Z.; Yang, W. Self-Consistent Calculation of the Localized Orbital Scaling Correction for Correct Electron Densities and Energy-Level Alignments in Density Functional Theory. *J. Phys. Chem. Lett.* **2020**, *11*, 10269–10277.
- (81) Mahler, A.; Williams, J.; Su, N. Q.; Yang, W. Localized Orbital Scaling Correction for Periodic Systems. *Phys. Rev. B* **2022**, *106*, 035147.
- (82) Mei, Y.; Yu, J.; Chen, Z.; Su, N. Q.; Yang, W. LibSC: Library for scaling correction methods in density functional theory. *J. Chem. Theory Comput.* **2022**, *18*, 840–850.
- (83) Yang, W.; Cohen, A. J.; De Proft, F.; Geerlings, P. Analytical evaluation of Fukui functions and real-space linear response function. *J. Chem. Phys.* **2012**, *136*.
- (84) Peng, D.; Yang, W. Fukui function and response function for nonlocal and fractional systems. *J. Chem. Phys.* **2013**, *138*.
- (85) Martin, R. M.; Reining, L.; Ceperley, D. M. *Interacting electrons*; Cambridge University Press, 2016.
- (86) Boys, S. F. Construction of some molecular orbitals to be approximately invariant for changes from one molecule to another. *Rev. Mod. Phys.* **1960**, *32*, 296.
- (87) Cohen, A. J.; Mori-Sánchez, P.; Yang, W. Fractional charge perspective on the band gap in density-functional theory. *Phys. Rev. B* **2008**, *77*, 115123.

- (88) Mei, Y.; Li, C.; Su, N. Q.; Yang, W. Approximating Quasiparticle and Excitation Energies from Ground State Generalized Kohn–Sham Calculations. *J. Phys. Chem. A* **2019**, *123*, 666–673.
- (89) Li, J.; Jin, Y.; Su, N. Q.; Yang, W. Combining localized orbital scaling correction and Bethe–Salpeter equation for accurate excitation energies. *J. Chem. Phys.* **2022**, *156*.
- (90) Golze, D.; Keller, L.; Rinke, P. Accurate absolute and relative core-level binding energies from GW. *J. Phys. Chem. Lett.* **2020**, *11*, 1840–1847.
- (91) Weigend, F.; Ahlrichs, R. Balanced basis sets of split valence, triple zeta valence and quadruple zeta valence quality for H to Rn: Design and assessment of accuracy. *Phys. Chem. Chem. Phys.* **2005**, *7*, 3297.
- (92) An in-house program for QM/MM simulations; available from <https://qm4d.org/>.
- (93) Keller, L.; Blum, V.; Rinke, P.; Golze, D. Relativistic correction scheme for core-level binding energies from GW. *J. Chem. Phys.* **2020**, *153*, 114110.